Chapter I

Dynamics and optical control of an individual Cr spin in a CdTe QD

We successfully included single Cr atom in CdTe quantum dot, and were able to probe them optically. We evidenced a strong spin-to-strain coupling for the Cr, particularly promising for the development of hybrid spin-mechanical systems and coherent mechanical driving. To be able to do these, the first key steps are the possibility to prepare and probe the spin of a single magnetic atom.

To probe the dynamics under excitation, we used photon correlation techniques. Auto-correlation of the photons emitted by the QD under continuous optical excitation reveals fluctuations of the localized spin with a timescale in the 10 ns range. Cross-correlation gives quantitative transfer time between Cr spin states.

In the second part, we demonstrate the possibility to prepare the Cr spin using resonant optical pumping. Monitoring the time dependence of the intensity of the resonant fluorescence of the quantum dot during this process permits us to probe the dynamics of the optical initialization of the Cr spin. Using resonant excitation, we measured a Cr spin relaxation time in the dark at $T = 5$ K in the μs range. Using this technique, we also identified a relaxation channel for the Cr spin via phonon-mediated h-Cr spin flip-flop, similar to the process described in Sec. III.2.3

Finally, we demonstrate that, under a resonant single-mode laser field, the energy of any spin state of an individual Cr atom can be independently tuned by using the optical Stark shift effect.

I.1 Probing the spin fluctuations of the Cr

The easiest way to look at the Cr spin dynamics under continuous wave (CW) optical excitation is to probe the statistics of time arrivals of the photons emitted

in a given PL peak. To do so, we used a Hanbury Brown and Twiss (HBT) setup to perform auto-correlation of the PL intensity of the different energy levels. In these start-stop experiments, the detection of the first photon indicates by its energy and polarization that the Cr spin has a given orientation. The probability of detection of a second photon with the same energy and polarization is proportional to the probability of conserving this spin state. For processes fast compared to the time scale of the experiment, this measure is a good approximation of the second order correlation function $g^{(2)}(\tau)$.

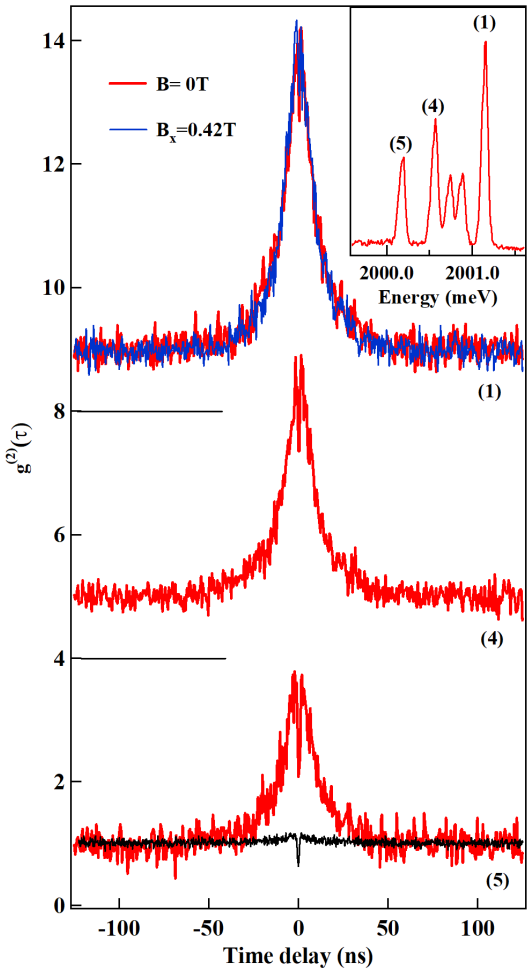

Figure I.1: Auto-correlation of the PL intensity collected in circular polarization on the X-Cr lines (1), (4) and (5) and compared with the auto-correlation of the exciton in a non-magnetic QD (black line). The curves are shifted for clarity. For line (1), the auto-correlation is also recorded under a transverse magnetic field $B_x = 0.42$ T (blue line).

The experiments were performed on QD2, as defined in Fig. IV.1, which spectra is reported in the inset of Fig. I.1. Its PL presents a clear splitting between each peaks, making the probing of a single state easier. Fig. I.1 shows $g^{(2)}(\tau)$ for the lines (1), (4) and (5) recorded in circular polarization. These signals are compared with

the auto-correlation obtained for the PL of a non-magnetic QD (black line) which is characteristic of a single-photon emitter with a dip (anti-bunching) at short delays. The width of the anti-bunching is given by the lifetime of the emitter and the generation rate of excitons and its depth is limited by the time resolution of the HBT setup. As illustrated in Fig. I.1, typical non-magnetic CdTe/ZnTe QDs do not present any significant bunching induced by charge fluctuations [1, 2]. A similar auto-correlation on a X-Cr PL line still presents a reduced coincidence rate near zero delay, but it is mainly characterized by a large photon bunching with a full width at half maximum (FWHM) in the 20 ns range. This large bunching reflects an intermittency in the emission of a given line of the QD coming from fluctuations of the Cr spin in a 10 ns timescale as it will be confirmed by cross-correlation measurements.

The amplitude of the bunching reaches 5 for line (1) and is slightly weaker for the lower energy lines. In a simple picture of blinking where the selected QD line can be either in a state ON or OFF, the amplitude of the bunching is given by Γ_{OFF}/Γ_{ON}, with Γ_{ON} the transition rates from OFF to ON, and Γ_{OFF} the one from ON to OFF [3]. An amplitude of bunching larger than 1 is then expected in a multilevel spin system where, after a spin relaxation, multiple spin-flips are usually required to come back to the initial state ($\Gamma_{ON} < \Gamma_{OFF}$). Let us finally note that the bunching signal is not affected by a weak transverse magnetic field ($B_x = 0.42$ T in Fig. I.1). This confirms the presence of a large strain induced magnetic anisotropy D_0 which splits the Cr and X-Cr states and blocks their precession in a magnetic field.

One should note that the observed spin dynamics depends on the optical excitation power. Increasing the excitation power significantly reduces the width of the bunching (Fig. I.2), linked to an increase of the Cr spin fluctuations. Within the X-Cr complex, the electron-Cr exchange interaction and the hole-Cr exchange interaction in the presence of heavy-hole/light-hole mixing can both induce spin-flips of the Cr. Though weak, the probability of such spin flips increases with the occupation of the QD with an exciton and dominates the spin dynamics in the high excitation regime required for the photon correlation measurements.

The excitation power dependence shows that the measured width of the bunching is not limited by the intrinsic Cr spin relaxation time τ_{Cr}. This gives a lower bound for τ_{Cr} in the 20 ns range. A shorter value would impose, at low excitation intensity, faster spin fluctuations than observed experimentally. The Cr spin relaxation time is ultimately controlled by the interaction with acoustic phonons and could depend on the optical excitation through the generation of non-equilibrium acoustic phonons during the relaxation of injected carriers [4, 5]. It is however expected to be longer than the observed dynamics [6] and cannot be determined with these measurements which require a large photon count rate.

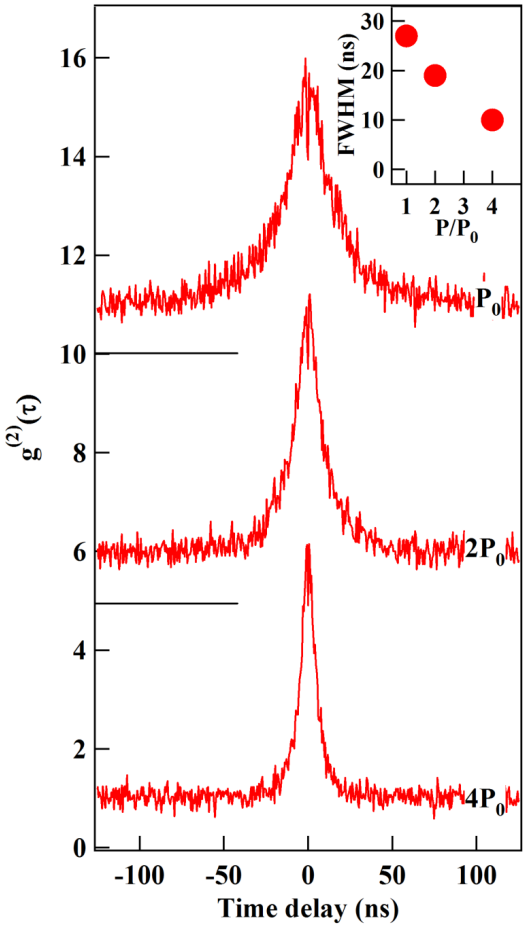

Figure I.2: Auto-correlation of the PL intensity recorded in circular polarization on the high energy X-Cr line (1) for different excitation powers. The inset shows the corresponding FWHM of the bunching signal versus excitation power.

To analyze more in detail the spin relaxation channels, cross-correlation measurements were performed on the PL emitted by the high energy and the low energy lines in the same circular polarization. The cross-correlation shows a large anti-bunching with a FWHM in the 10 ns range and $g^{(2)}(0) \approx 0.3$ (Fig. I.3(a)). Whereas the auto-correlation probes the probability for the Cr spin to be conserved, this cross-correlation is a probe of the spin transfer time between the spin states $S_z = +1$ and $S_z = -1$. As for the auto-correlation, the cross-correlation strongly depends on the excitation power. At weak excitation, a spin transfer time of about 20 ns is observed. It is accelerated with the increase of the excitation power (Fig. I.3(a)). This transfer time could be controlled by anisotropic in-plane strain which couples Cr spin states separated by two units through an additional term $E(S_x^2 - S_y^2)$ in the Cr fine structure Hamiltonian [7]. However, even at low excitation power, the measured transfer time is not affected by a longitudinal mag-

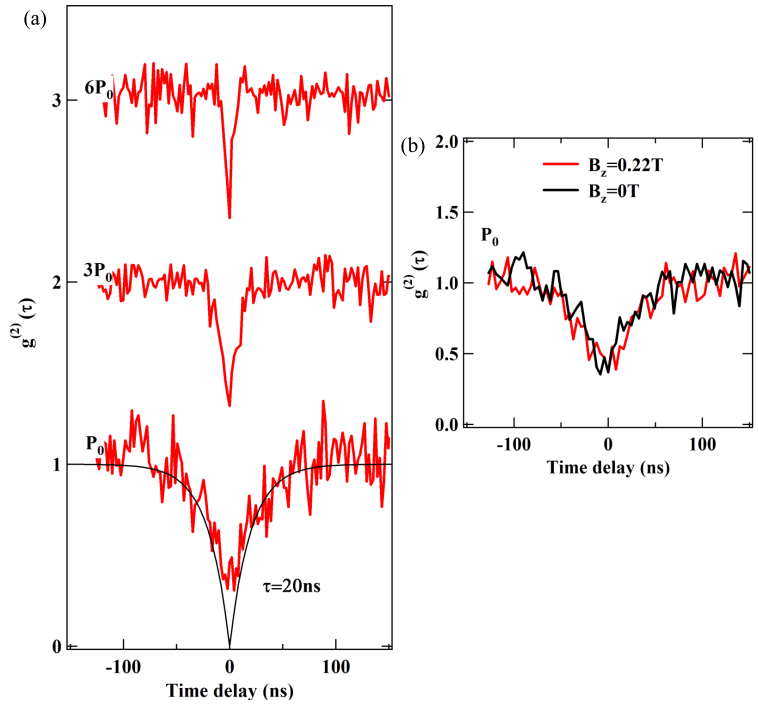

Figure I.3: (a) Correlation signal of the PL intensity of lines (1) and (4) recorded in the same circular polarization (cross-correlation) for three different excitation powers. The curves are shifted for clarity. The black line is an exponential fit with a characteristic time $\tau = 20$ ns. (b) Longitudinal magnetic field dependence of the cross-correlation signal obtained at low excitation power.

netic field (Fig. I.3(b)). This shows that for such QD the strain anisotropy term E is weak and is not the main parameter controlling the transfer time between the states $S_z = \pm 1$. The spin transfer time is dominated by spin-flips induced by the exciton/Cr interaction.

This fast transfer time is an indication of efficient carrier-Cr spins flip-flop, an interaction with phonons, or both. However, it is hard to extract precise informations from the auto-correlation and cross-correlation experiments only. In order to delve into more details, we have to use more precise tools.

I.2 Resonant optical pumping of a Cr spin

Another way to probe the spin dynamic of a Cr-doped QD under excitation is to prepare the Cr spin in a given state and monitor its evolution. To do so, we put a laser in resonance one of the transition of the QD, pumping the Cr in the selected

state: an exciton can only be injected in if the Cr spin is in the resonantly excited state. If the intraband relaxation time of the X-Cr complex is smaller than the one of the Cr alone ($\tau_{Cr} > \tau_{X-Cr}$), the Cr may undergo spin-flips after an absorption, progressively decreasing the population of the resonantly excited state. Once it is empty, the resonant laser cannot injects exciton in the QD anymore. A signature of the pumping can be detected by looking at the cross-polarized PL of the dot after a spin-flip of the exciton. It supposes that the spin flip time of the exciton in presence of Cr is smaller than the relaxation time of the Cr in the excited state τ_{X-Cr}. This process is illustrated on the inset of Fig. I.4 for an excitation toward $|S_z = +1, X_z = +1\rangle$ state.

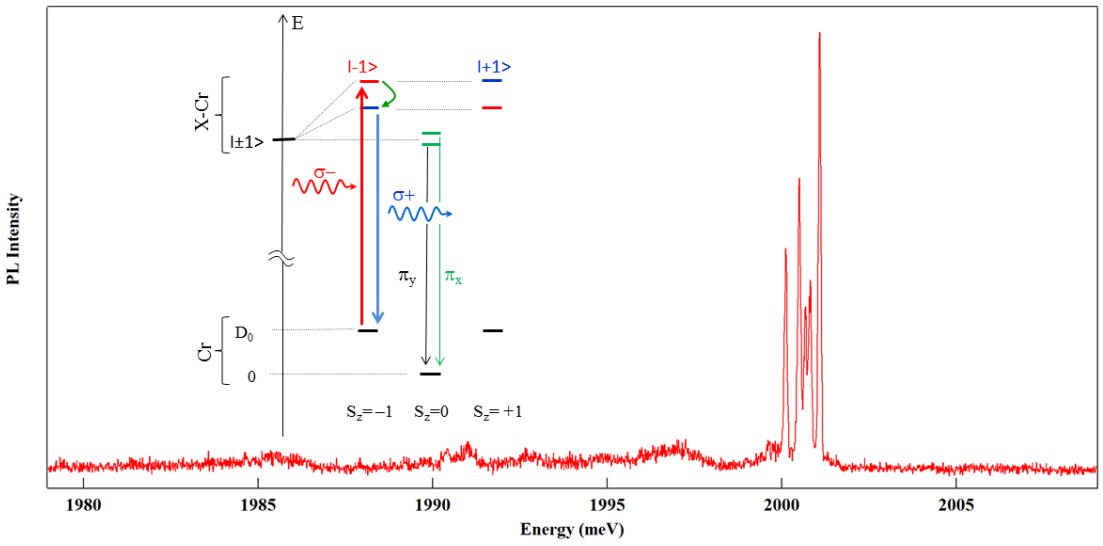

Figure I.4: Low temperature PL spectra of QD2 exciton in cross-lineraly polarized excitation and detection for B = 0T. No contribution of the charge excitons was found. Inset: Schematic of the energy levels in a Cr-doped QD and configuration of excitation/detection for resonant optical pumping.

To initialize and read-out the Cr spin, we developed a two wavelengths pump-probe experiment. A circularly polarized single mode laser (*resonant pump*) tuned on a X-Cr level is used to pump the Cr spin (i.e., empty the spin state under resonant excitation). Then, a second laser, tuned on an excited state of the QD (*quasi-resonant probe*), injects excitons independently of the Cr spin S_z and drives the Cr to an effective spin temperature where the three ground states $S_z = 0, \pm 1$ are populated [7]. By recording the PL of a X-Cr lines in circular polarization under this periodic sequence of excitation, we can monitor the time evolution of the population of a given Cr spin state.

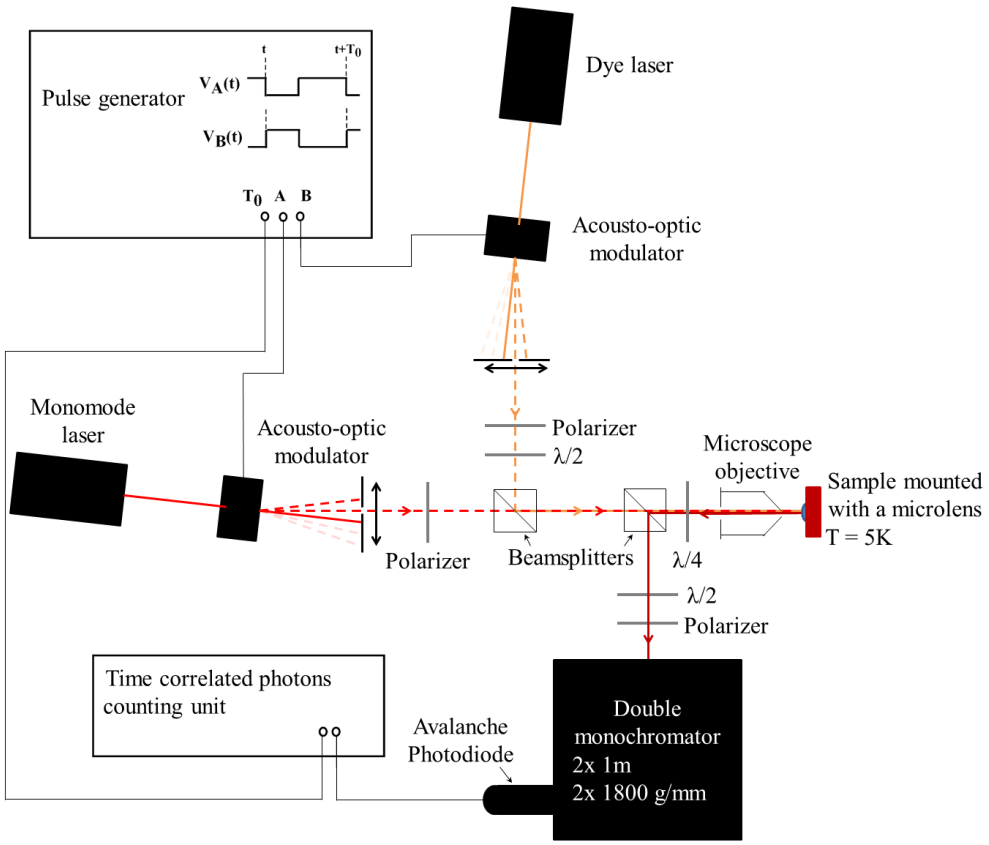

Figure I.5: Schematic view of the micro-spectroscopy set-up used for the time-resolved optical pumping experiment. The monomode laser is a dye laser tuned on resonance with the studied dot transition, acting as the pump. The other dye laser is tuned on a resonant state at $E_{probe} = 2070$ meV, acting as the probe. Both beamsplitters are non-polarizing.

Fig. I.5 shows our experimental set-up. Both of the continuous wave (CW) lasers passed through accousto-optic modulators, going ON and OFF in sequences as illustrated at the bottom of Fig. I.6 (a). The modulators take about 10 ns to go from OFF to ON. Following them, a diaphragm is centered on the first diffraction spot created by the modulators. This creates a train of pulses of tunable duration, alternating between the pump and the probe. This two lasers are focused on the sample with a microscope objective. A high index ($n \approx 2.5$) Solid Immersion Lens (SIL) is also mounted on the sample surface, to increase the surface resolution and the collection of photons emitted by the QD. The emitted light pass through a monochromator and is then collected with an avalanche photodiode with a time resolution of about 350 ps.

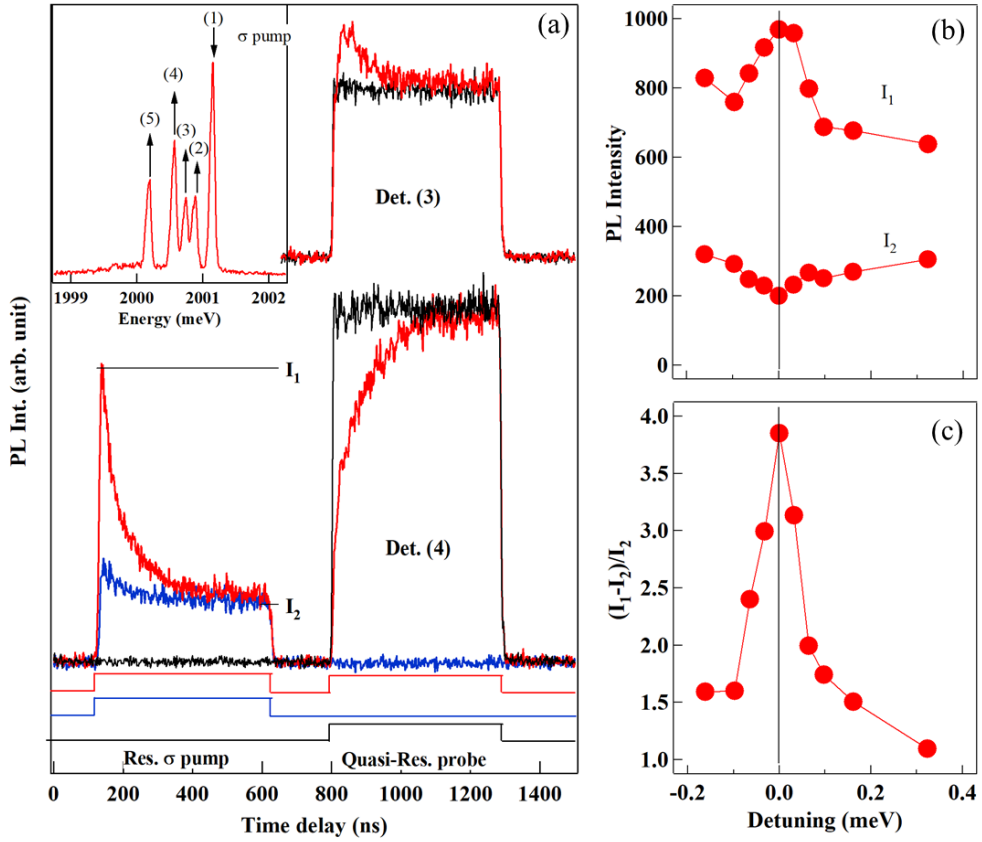

Figure I.6: (a) PL transients recorded in circular polarization on line (3) and on line (4) (as defined in the inset) under the resonant (pump on (1)) and quasi-resonant optical excitation sequences displayed at the bottom. Inset: PL of X-Cr and configuration of the resonant excitation and detection. (b) and (c): Energy detuning dependence of resonant PL intensity (I_1, at the beginning and I_2, at the end of the pump pulse) and of the corresponding normalized amplitude of pumping transient $\Delta I/I_2 = (I_1 - I_2)/I_2$.

The main features of the optical pumping experiment are presented in Fig. I.6 (a). The QD is excited on the high energy state of X-Cr with $\sigma-$ photons (X-Cr state $|S_z = -1, -1\rangle$), only creating an exciton in the dot if the Cr spin is $S_z = -1$. After this pumping sequence, the resonant pump is switched off and followed by the non-resonant probe.

A clear signature of the optical pumping appears on the time evolution of the PL intensity of the low energy bright exciton line (4). The PL of this line during the probe pulse, recorded in opposite circular polarization with the resonant pump, depends on the population of $S_z = -1$. It strongly differs between the two pump-

probe sequences, where the resonant pump is either on or off. The difference of intensity at the beginning of the probe pulse is a measurement of the efficiency of the pumping. The PL transient during the probe pulse corresponds to a destruction of the non-equilibrium population distribution prepared by the pump. As expected for an increase of the Cr spin temperature, the population of the ground spin state $S_z = 0$ also decreases during the probe pulse. This decrease directly appears in the time evolution of the amplitude of the central X-Cr lines during the probe pulse (Det. (3) in Fig. I.6 (a)). The increase of the population of $S_z = 0$ during the probe pulse shows that the population of $S_z = -1$ has been partially transferred to $S_z = 0$ during the resonant pumping sequence. This is described in more details in Sec. I.3.2.

A more direct way to probe the optical pumping speed and efficiency is to monitor the time evolution of the PL during the resonant excitation by the pump pulse. Under resonant excitation on the high energy X-Cr line, an exciton spin-flip with conservation of the Cr spin can produce a PL on the low energy line [8]. This experiment configuration is illustrated in the inset of Fig. I.4. In this process, the exciton flips its spin by emitting (or absorbing) an acoustic phonon. Such spin-flip is enhanced by the large acoustic phonon density of states at the energy of the inter-level splitting induced by the exchange interaction with the Cr spin which act as an effective magnetic field [9, 10]. The resulting weak resonant PL signal depends on the occupation of the Cr state $S_z = -1$ and is used to monitor the time dependence of the spin selective absorption of the QD.

The time evolution of the PL of the low energy line of X-Cr under an excitation on the high energy line is presented in Fig. I.6 (a) for two different pump-probe sequences: probe on and probe off. When the probe laser is on, a large effective Cr spin temperature is established before each pumping pulse. The amplitude of the resonant PL is maximum at the beginning of the pump pulse (I_1) and progressively decreases. A decrease of about 80% is observed with a characteristic decay time in the tens of ns range. When the probe laser is off, the initial amplitude of the PL transient during the pump pulse is significantly weaker. This decrease is a consequence of the conservation of the out of equilibrium Cr spin distribution during the dark time between two consecutive pumping pulses.

The steady state resonant PL intensity reached at the end of the pump pulse (I_2) depends on the optical pumping efficiency which is controlled by the ratio of the spin-flip rate for the Cr spin in the exchange field of the exciton and the relaxation of the Cr spin in the empty dot. However, even with cross-circularly polarized excitation/detection, this steady state PL can also contain a weak contribution from an absorption in the acoustic phonon sideband of the low energy line [11]. Fig. I.6 (b) presents the amplitude of the resonant PL detected on the low energy line for a detuning of the pump around the high energy line. A res-

onance is observed in the initial amplitude I_1 of the PL. It reflects the energy dependence of the absorption of the QD. A small decrease of the steady state PL I_2 is also observed at the resonance. As displayed in Fig. I.6 (c), the corresponding normalized amplitude of the pumping transient, $(I_1 - I_2)/I_2$, presents a clear resonant behaviour demonstrating the excitation energy dependence of the optical pumping process. The width of the resonance ($\sim 100\mu eV$) is the width of the QD's absorption broadened by the fluctuating environment [12].

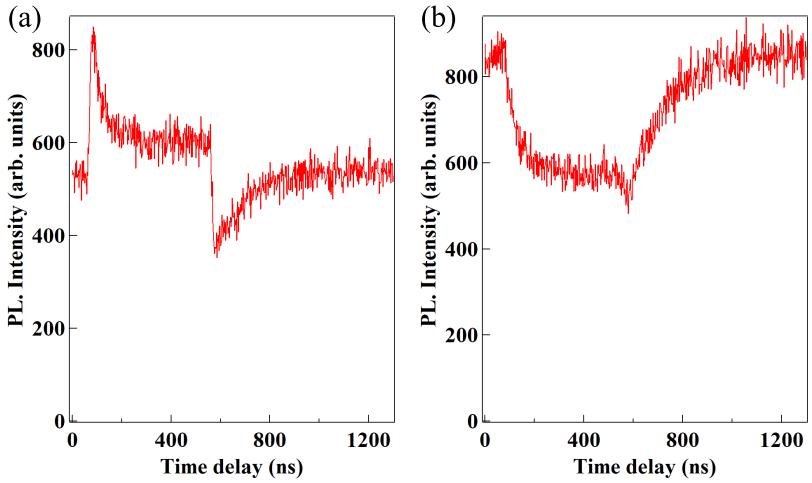

Figure I.7: Optical pumping under a CW probe at $E = 2004$ meV. (a) Pumping on line (1) and detecting on line (4). (b) Pumping on line (4) and detecting on line (1).

A signature of the optical pumping can also be observed without modulating the probe (probe ON all the time). We did the experiment in two configurations, presented on Fig. I.7: either exciting resonantly on line (1) (corresponding to the state $|S_z = -1, X_z = -1\rangle$ when exciting in $\sigma-$ polarization) and detecting on line (4) (corresponding to the state $|S_z = -1, X - z = +1\rangle$), or the opposite. The signal was detected in σ_{cross} configuration. When the pump pulse is turned on the high energy peak, we can see the same transients as shown in Fig. I.6 (a): a first, quick increase followed by a slower decrease. The pumping transient seems smaller due to the high background signal created by the continuous probe. When the pulse is turned off, the PL decreases quickly, followed by a slow increase during about 200 ns before coming back at the intensity it has before the pumping. This is the same transient as the one observed on the probe pulse in Fig. I.6 (a).

The complimentary evolution happens when we pump on the line (4) and detect on line (1). In this case, when the pumping laser is turned on, we first observe a decrease about 100 ns long, corresponding to the pumping of the state

$S_z = -1$. No increase of intensity is detected because the resonantly excited state ($|S_z = -1, X_z = +1\rangle$) is at lower energy than the the monitored state ($|S_z = -1, X_z = -1\rangle$). Therefore, no population transfer can occur between these states, and the observed decrease correspond to the state $S_z = -1$ being emptied. Once the pumped state is emptied, the signal stabilize at low intensity. The remaining signal is due to the non-resonant probe injecting exciton independently from the Cr spin. The PL intensity then decreases slightly when the pump pulse finish, and then increasing slowly in a 200 ns timescale, when the population is restored by the non-resonant laser, caused by the same process as the second transient on Fig. I.7 (a).

We demonstrated the possibility to optically pepare the spin of a Cr atom embedded in a QD via resonant optical pumping, and the ability to probe the pumped Cr state after a exciton spin-flip. This preparation can be used to study the dynamic of the Cr spin in different configuration, and open the possibility to study other phenomena than the auto-correlation alone.

I.3 Dynamics of a Cr spin under optical excitation

We begin looking at the evolution of the pumping and heating transients with the power of their respective laser. With the autocorrelation, it is another probe of the dynamic of the X-Cr system under excitation.

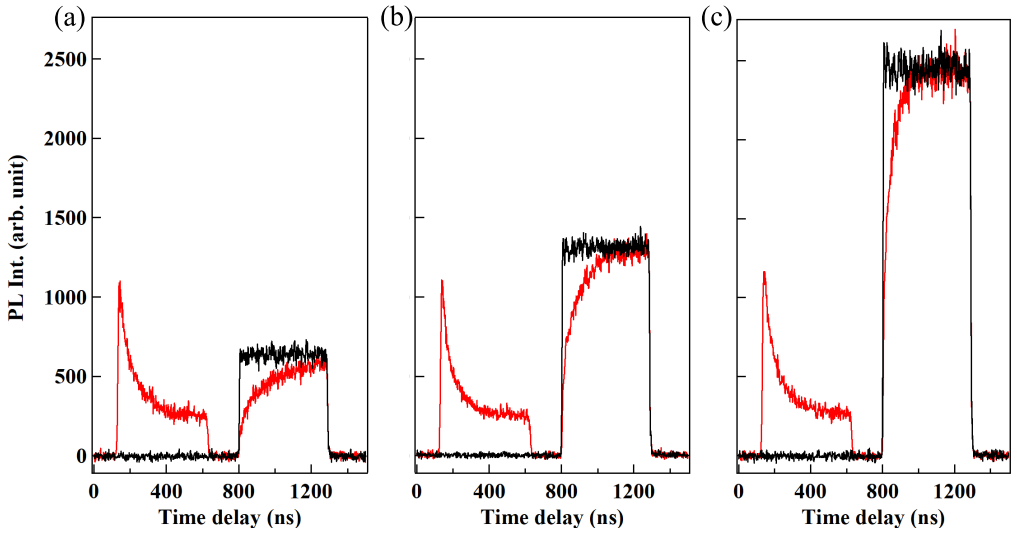

Figure I.8: PL transients measured on line (4) while pumping on line (1) at $P_{pump} = 250$ μW (red) or without pumping (dark). (a) $P_{probe} = 125$ μW. (b) $P_{probe} = 250$ μW. (c) $P_{probe} = 500$ μW.

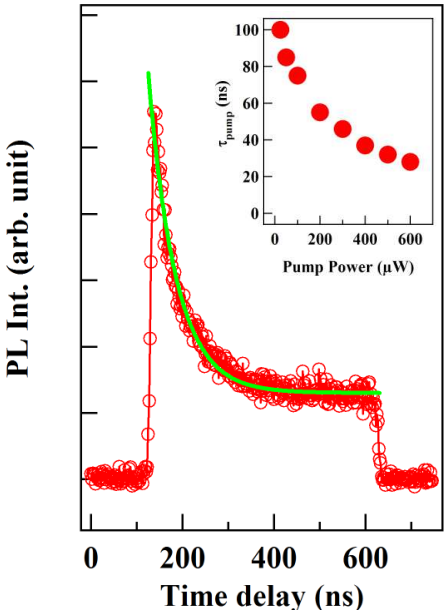

Figure I.9: Detail of the PL transient measured during the resonant pump pulse on line (1) for a power $P_{probe} = 250$ μW. The detection was done on line (4). The exponential fit (green) gives a characteristic time of $\tau_{pump} = 60$ ns. The inset presents the evolution of τ_{pump} as a function of the pumping laser power.

We began to study the evolution of the heating transient with the probe laser. The results are presented on Fig. I.8. The first noticeable evolution is the increase of the PL intensity during the probe pulse, proportional to the increase of the probe power. A higher power lead to a higher probability of injecting an exciton in the QD. Therefore, more photon will be emitted by the dot, proportionally to the laser power, as long as there is no contribution of the biexciton.

More interestingly, we observe that the speed of this spin heating process depends on the intensity of the probe laser. The probe pulse last for about 500 ns, and, for a laser power of 125 μW, the nonequilibrium population distribution is not completely destroyed at the end of it (Fig. I.8 (a)). The transient reduces to about 200 ns for a laser power of 500 μW. This speeding of the heating process is also controlled by the higher rate of carriers injection. The heating is done by the interaction between the excitons and the Cr spin. The probe inject excitons at high energy in the QD, interacting with the Cr independently of its spin state. A higher number of injected high energy carriers therefore leads to a quicker destruction of the nonequilibrium state created by the pump pulse.

Study of the evolution of the pumping transient as a function of the pumping laser power was also done, and the results are presented on Fig. I.9. As expected for a spin optical pumping process, the characteristic time of the PL transient decreases with the increase of the pump laser intensity (inset of Fig. I.9) [8]. This transient is akin to the autocorrelation discussed in Sec. I.1: it measures the time it takes for the X-Cr to exit the excited state. With a higher intensity laser, there is an exciton in the QD more often, and since $\tau_{X-Cr} > \tau_{Cr}$, the system relax

faster. However, it is hard to extract value from this, such as it was with the autocorrelation.

I.3.1 Optical pumping induced by h-Cr flip-flop

We saw in Sec. I.2 that the population of the resonantly prepare $S_z = -1$ state can be transferred to $S_z = 0$. The was evidenced by the appearance of a transient at the beginning of PL of the probe pulse taken on line (3) when the resonant laser was turned on. In order to study this transfer, we performed resonant optical excitation of the state $S_z = -1$, while detecting on an emission line associated with the state $S_z = 0$.

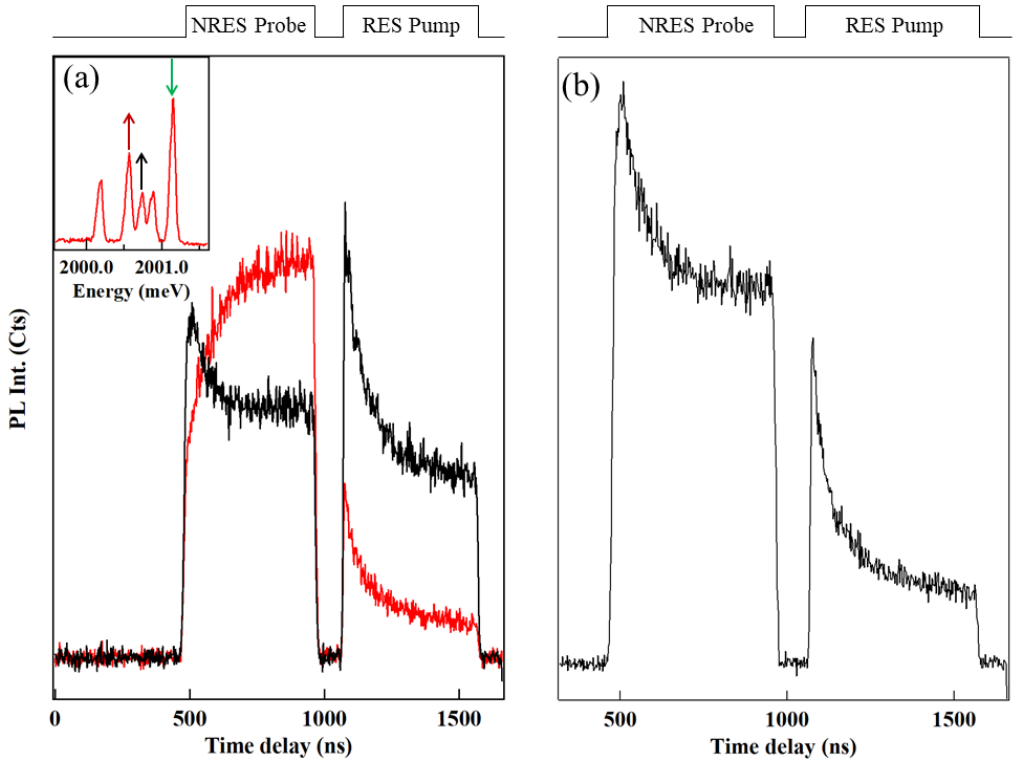

Figure I.10: (a) Pumping experiment at T= 5 K in circular polarization exciting on line (1) and detecting either on line (3) (black) or on line (4) (red). The inset presents the experiment configuration, with the excitation shown as a green arrow and the detection as red and black arrows. (b) Pumping experiement at T= 5 K in linear polarization, detecting on line (3).

Fig. I.10 (a) shows the PL detected during the probe and pump pulse on the low energy line in red and in the central peak in black. The detection on the low

energy line is similar to the one presented in Fig. I.6. It was reported here for comparison with the evolution of the state $S_z = 0$.

As noticed previously, during the probe pulse, the central peak shows a quick increase followed by a slow decrease, lasting for about 250 ns. This intensity decrease contrasts with the increase observed when detecting on the line (4): the increase shows the reconstruction of the state, while the decrease shows that the state is being destroyed. It suggests that, when emptying a pumped state, some of the population have transferred to $S_z = 0$. When heating with the non-resonant pulse, this state is partially emptied and the thermal equilibrium is restored.

A clearer signature of the preparation of state can be seen during the pump pulse. There again, a quick increase is first seen, before a decrease of the PL intensity. However, the PL stays at high intensity even at the end of pumping pulse. This large remaining signal is due to the contribution of the peak phonon band when exciting in circular polarization. In order to get rid of this contribution, we did the same experiment in linear polarization, detecting in cross linear configuration. However, doing so, we cannot excite selectively one transition, since both the excitons $X_z = +1$ and $X_z = -1$ can be injected under such an excitation. Therefore, we are exciting a linear combination of the states $|S_z = +1, X_z = +1\rangle$ and $|S_z = -1, X_z = -1\rangle$. Nonetheless, a high intensity transient is observed at the beginning of both the probe pulse and the pump pulse. This shows that, when a high energy state is pumped, part of the population may relax toward the state $S_z = 0$.

This relaxation can be explained by a hole-Cr spins flip-flop in the excited state, such as the one presented for the hole-Mn pseudo-spin relaxation in Sec. III.2.3. As with the Mn, the non-diagonal term of the hole-Cr exchange interaction mixes the heavy holes and the light hole. The perturbed $|S_z = 0, X_z = +1\rangle$ state can be written:

$$|0\rangle|\widetilde{\Uparrow_h, \downarrow_e}\rangle = |0\rangle|\Uparrow_h, \downarrow_e\rangle - \frac{\sqrt{18}}{2}\frac{I_{hCr}}{\Delta_{lh}}|+1\rangle|\uparrow_h, \downarrow_e\rangle \tag{I.1}$$

Moreover, one can notice that the $|S_z = 0, X_z = +1\rangle$ state is only one hole-Cr spin flip-flop away from the dark state state $|S_z = +1, X_z = -2\rangle$. This one can be written:

$$|+1\rangle|\widetilde{\Downarrow_h, \downarrow_e}\rangle = |+1\rangle|\Downarrow_h, \downarrow_e\rangle - \frac{\sqrt{18}}{2}\frac{I_{hCr}}{\Delta_{lh}}|0\rangle|\downarrow_h, \downarrow_e\rangle \tag{I.2}$$

The effects of phonons can be seen by interfacing those two states through the Bir-Pikus hamiltonian $\mathcal{H}_{BP}$, described in Eq. I.24. The phonon induced deformation comes into play through the off-diagonal term of the hamiltonian. The phonon-mediated coupling between $|0\rangle|\widetilde{\Uparrow_h, \downarrow_e}\rangle$ and $|+1\rangle|\widetilde{\Downarrow_h, \downarrow_e}\rangle$ can then be

found through the hamiltonian term:

$$\langle \Downarrow_h, \widetilde{\downarrow_e} \, | \langle +1 | \mathcal{H}_{BP} | 0 \rangle | \, \widetilde{\Uparrow_h, \downarrow_e} \rangle = 2 \times \left(-\frac{\sqrt{18}}{2} \frac{I_{hCr}}{\Delta_{lh}} \right) \times r^* \tag{I.3}$$

with r^* as defined in Eq. I.55.

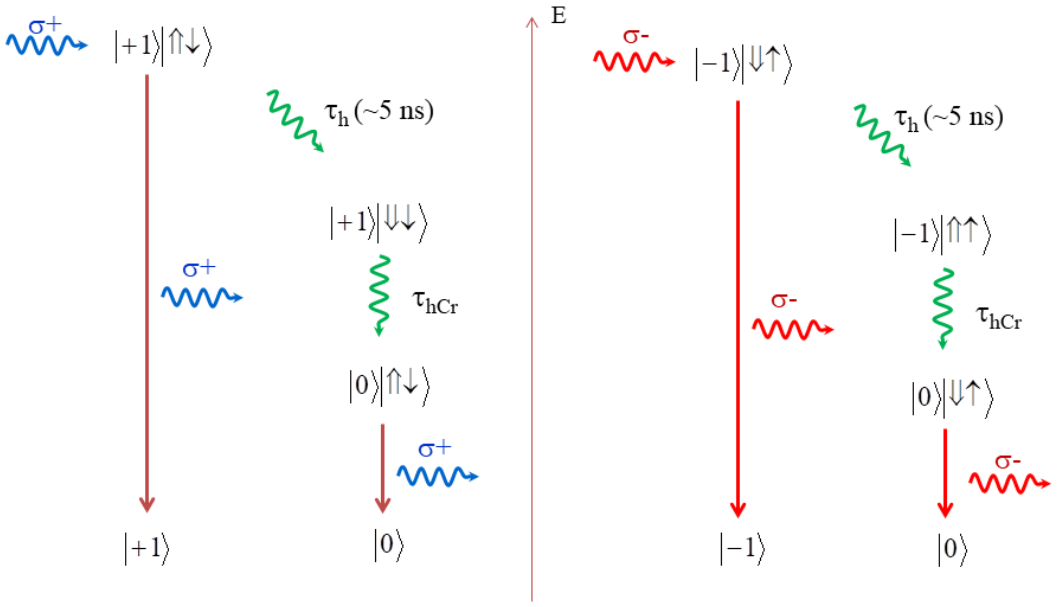

Figure I.11: Relaxation paths for the X-Cr system, starting either on the $|S_z = +1, X_z = +1\rangle$ state and finishing on the $|S_z = 0, X_z = +1\rangle$ one, or starting on the $|S_z = -1, X_z = -1\rangle$ state and finishing on the $|S_z = 0, X_z = -1\rangle$ one, after a hole flip followed by a hole-Cr flip-flop mediated by phonons.

However, the closest state that can be resonantly excited is $|S_z = +1, X_z = +1\rangle$. To reach $|S_z = +1, X_z = -2\rangle$, a spin flip of the hole has to occur first. In CdTe quantum dot, this spin flip was found to occur with a characteristic time $\tau_h = 5$ ns. Once it happens, the system can emit a phonon to relax from $|S_z = +1, X_z = -2\rangle$ to $|S_z = 0, X_z = +1\rangle$. This same process can be devised for a resonant excitation toward $|S_z = -1, X_z = -1\rangle$. The hole flip will then bring the system to $|S_z = -1, X_z = +2\rangle$, from which it can do a phonon-mediated relaxation toward $|S_z = 0, X_z = -1\rangle$. Those two processes are illustrated on Fig. I.11.

The same steps done in Sec. III.2.3 can be followed here to find the characteristic time τ_{hCr} of the phonon-mediated relaxation as a function of the splitting between the two states. The resulting curve is drawn on Fig. I.12. A bright exciton - dark exciton splitting in the meV is expected for Cr in SK dots. It gives a τ_{hCr} of a few ns, which is coherent with the fast state preparation observed in Fig. I.10.

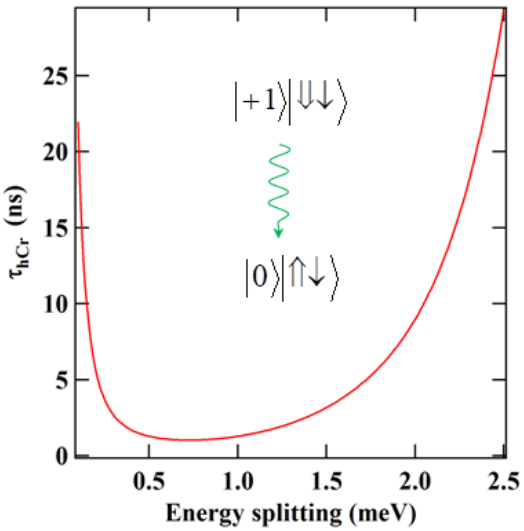

Figure I.12: Relaxation time τ_{hCr} between the states $|S_z = \pm 1, X_z = \mp 2\rangle$ and $|S_z = 0, X_z = \pm 1\rangle$, calculated at a temperature T = 7 K with the gaussian hole wave function parameters $l_z = 1.2$ nm and $l_\perp = 3$ nm, and the parameters $I_{hCr} = 0.25$ meV and $\Delta_{lh} = 25$ meV.

I.3.2 Cr heating by non-equilibrium phonons?

We saw that Cr spin is really sensible to the strain state. Therefore, it might be possible to act on the spin state of the atom through phonons. To test this, we tried replacing the carrier injection done by the heating pulse with pure phonons injection. Two experiments were performed, presented in Fig. I.13: heating the sample either away from the dot, or at a wavelength not absorbed neither by the QD nor the barriers.

We first put the heating laser away from the QD. Shining the probe laser 4 μm from the dot, we took the time resolved PL with (red) or without (black) the probe pulse. At this distance, the probability for an optically injected carrier to reach the QD is low. As shown on the pulse cycle above the picture, the non-resonant probe is turned on between 400 and 800 ns. No PL was detected during the probe pulse (Fig. I.13 (b)), showing that no exciton was injected during it. However, a strong effect is seen on the pumping transient of the resonant pump, with a normalized intensity more than 3 time more intense when the probe pulse is turned on. A study of the pumping transient intensity as a function of the probe laser power is done in Fig. I.13 (c). The normalized intensity $\Delta I/I_2$ increases with the laser power, stabilizing around 2.3 for probe power $P_{probe} > 300$ μW. This is coherent with a heating via phonons emitted by the probe. A more intense laser injects a greater amount of phonons in the sample, heating the Cr spin more efficiently. The pumping transient is thus more intense for a more intense probe pulse.

We also studied the evolution of the pumping transient normalized intensity as a function of the distance between the the pumping laser and the probe laser.

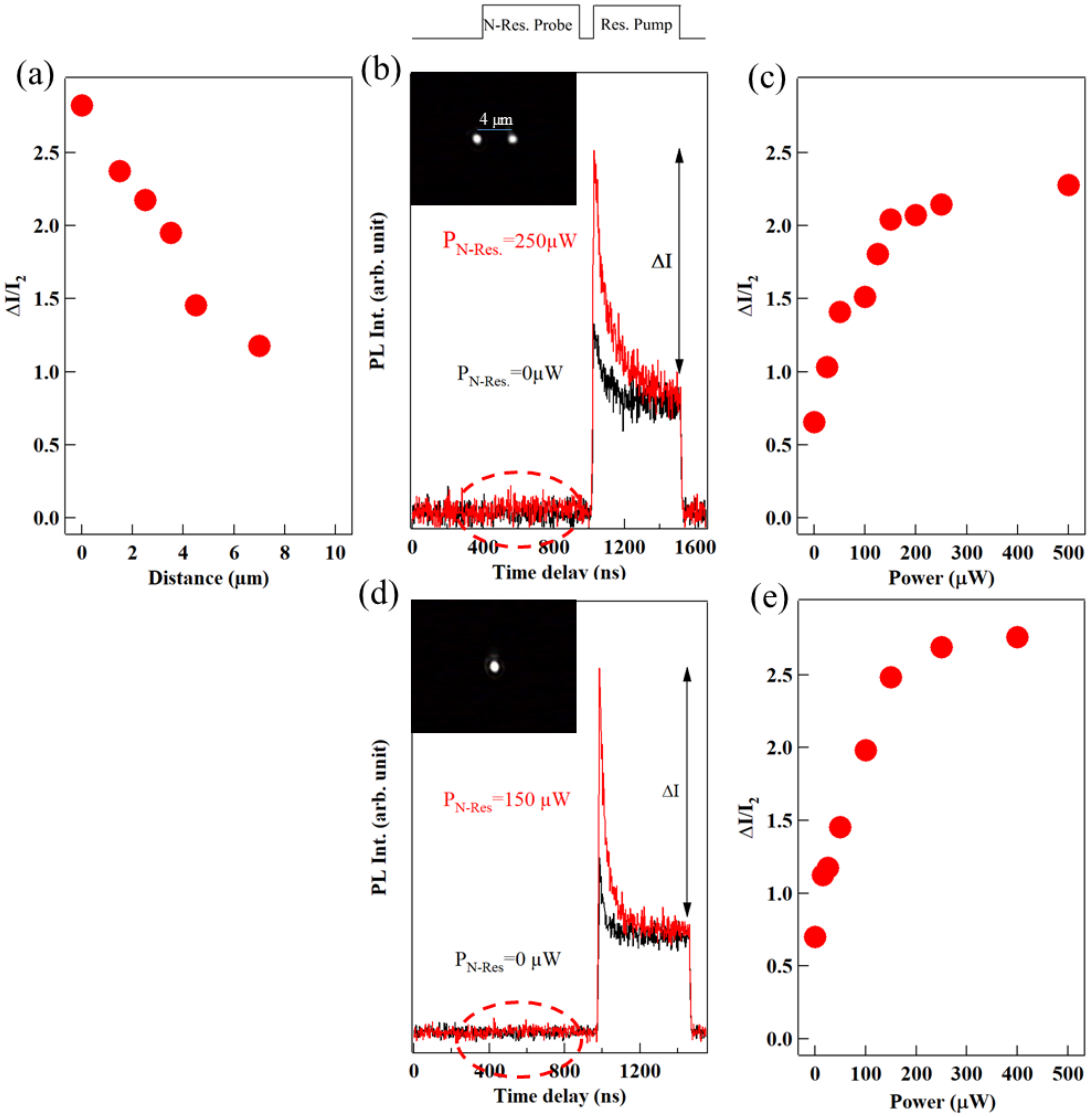

Figure I.13: (a) Evolution of the pumping transient intensity in a pump-probe experiment as a function of the distance between the probe laser and the dot. (b) PL transients recorded for a probe laser at $d = 4$ μm of the dot. Red: probe on; black: probe off. (c) Evolution of the pumping transient intensity as a function of the probe power, for a probe laser at $d = 4$ μm of the dot. (d) PL transient recorded for a probe laser at $E_{probe} = 2010$ meV. Red: probe on; black: probe off. (e) Evolution of the pumping transient intensity in function of the probe power, for a probe not absorbed nor by the QD neither in the barriers.

In a simple picture, phonons are created in the sample in a sphere centred at the position of the probe laser. When pulling aside the two laser spots, the QD will occupy a smaller surface on the phonons sphere. Less phonons will reach it, making the heating process less efficient. A diminution of the normalized intensity with the distance is then expected. We observe this in our experiment, as presented on the Fig. I.13 (c).

In the second configuration, the probe laser was put back at the QD position. We lowered its energy at $E_{probe} = 2010$ meV. This energy corresponds to a transparent state of the sample, where the energy could not be absorbed neither by the dot, nor by the barriers. The only source of heating are the phonons. Once again, a stronger pumping transient is observed when the heating pulse is turned on than without it. No PL was observed during the non-resonant pulse either (Fig. I.13 (d)). We performed a systematic study of the normalized intensity of the transient as a function of the probe power (Fig. I.13 (e)). It stabilizes at about 2.8 for a pumping power $P_{probe} = 200$ μW. This normalized intensity at high laser power higher than for a heating pulse far from the dot may come from the higher density of phonons injected by a laser at the dot position.

These measurements can be explained by the interaction between the Cr spin and the phonons created by the laser in the semiconductor. However, carriers might still be injected in the QD by the heating pulse. If the injected carrier density is low enough, no PL might be detected, but even this low density of carriers can be enough to heat the Cr spin. Therefore, those experiments are not enough to conclude definitively on the effects of phonons on the spin dynamic. More experiments are needed to assess their action.

I.4 Cr spin relaxation in the dark

Using resonant optical pumping technique presented in Sec. I.2 to prepare and read-out the Cr spin, we performed pump-probe experiments to observe its relaxation time in the absence of carriers (Fig. I.14). A non-equilibrium distribution of the Cr spin population is prepared with a circularly polarized resonant pump pulse on the high energy X-Cr line. The pump laser is then switched off, and switched on again after a dark time τ_{dark}. The amplitude of the pumping transient observed on the resonant PL of the low energy line depends on the Cr spin relaxation during τ_{dark}. As presented in Fig. I.14 (b), the amplitude of the transient is fully restored after a dark time of about 10 μs showing that after this delay the Cr spin is in equilibrium with the lattice temperature (T = 5 K). Let us note, however, that the initial amplitude of the pumping transient in this case is weaker than the one observed after a non-resonant probe pulse (Fig. I.6 (a)). This means that the non-resonant optical excitation drives the Cr spin to an effective temperature much

larger than the lattice temperature.

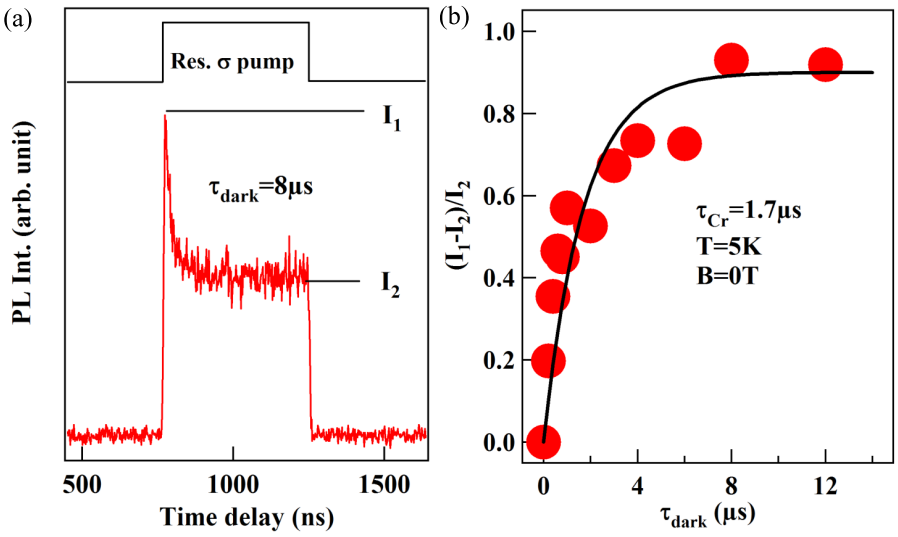

Figure I.14: (a) Time evolution of the PL intensity of line (4) of X-Cr under resonant excitation on line (1) with a circularly polarized excitation pulse. (b) Evolution of the amplitude of the pumping transient $\Delta I/I_2$ as a function of the dark time between the excitation pulses. The black line is an exponential evolution with a characteristic time $\tau_{Cr} = 1.7$ μs

From the time delay dependence of the amplitude of the transient, we deduce a Cr relaxation time $\tau_{Cr} \approx 1.7$ μs at B= 0 T and T= 5 K. For such neutral QD and in the absence of optical injection of carriers, this spin relaxation is likely to be controlled by the spin-lattice interaction. Despite the large spin-phonon coupling expected for this magnetic atom with an orbital momentum and a strain induced spin splitting in the meV range [7], the Cr spin relaxation time remains in the μs range. This spin memory is long enough for a practical use of Cr in an hybrid spin nano-mechanical system and could even be improved in different QDs structures with weaker biaxial strain [13], lower magnetic anisotropy splitting and consequently less coupling with acoustic phonons [6].

The Cr spin-flip time found for a relaxation in the dark (microseconds range) is a lot longer than the one found under optical excitation (tens of nanosecond range, see Sec. I.2). The fast Cr spin-flip under optical excitation can be due to the interaction with carriers (exchange induced Cr spin flips [6]) but can also be induced by the interaction with non-equilibrium acoustic phonons created during the energy relaxation of the injected carriers. Both mechanisms probably contribute to the Cr spin heating.

Another configuration to probe the relaxation of the Cr spin in the dark is

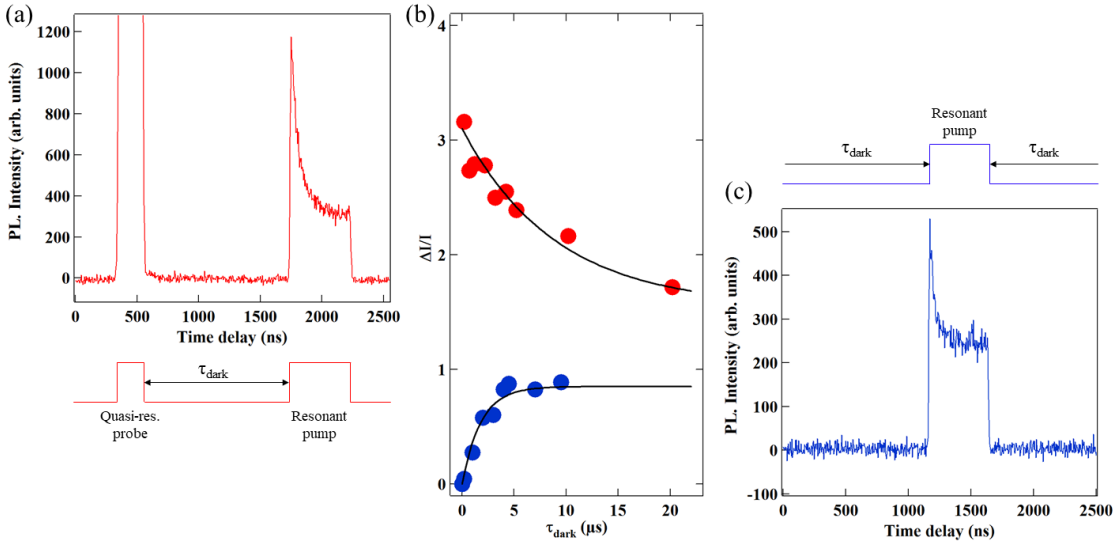

Figure I.15: Comparison of the relaxation of the Cr spin after resonant pumping in the line (1) with (red) or without (blue) a probe pulse ($E_{probe} = 2070$ meV). (a) Time resolved PL of line (4) for a resonant pump on line (1) with a probe pulse. (b) $\Delta I/I_2$ in function of the dark time τ_{dark} measured for the relaxation between the probe and the pump pulses (red) or between two pump pulses (blue). (c) Time resolved PL of line (4) for a resonant pump on line (1) with no probe pulse.

presented on Fig. I.15. In this configuration, the probe pusle is ON, and a dark time is introduced between the probe and the pump, leaving some time for the Cr spin to relax. We observe the most intense transient for $\tau_{dark} \approx 0$ μs, more intense than the transient of the pump alone after a long dark time, due to the higher spin temperature created by the probe pulse. The transient normalized intensity decreases when the dark time is getting longer. However, even after 20 μs of dark time, the transient normalized intensity is still about two times higher than the value at total relaxation for the pump alone, reached after a dark time of only 10 μs. It shows that the Cr remains at high temperature for a long time, even after the probe pulse went off. A τ_{Cr} of about 10 μs was found for the relaxation after the probe pulse.

This difference can be caused by the interaction with carriers injected by the probe or by the interaction with accoustic phonons, as discussed in Sec. I.3.2. The effect lasting for more than 20 μs suggests that the cause of this change of dynamics might be the interaction with phonons, since the carriers have a short lifetime in the quantum dot (in the range of 0.1 ns).

I.5 Optical Stark effect on an individual Cr spin

I.5.1 Dressed atom picture and Autler-Townes splitting

The resonant optical excitation on a X-Cr line can also be used to tune the energy of any Cr spin state through the optical Stark effect [14–16]. When a laser is put on resonance with a QD transition, a coupling is created between the laser photons and the resonantly excited quantum dot levels. The photons of the laser field are coherently absorbed by the ground state and emitted by the excited state at a Rabi flopping frequency Ω_r, depending on the strength of the coupling between the laser field and the transition dipole. For a n photon state of the control laser, the unperturbed states $|Cr\rangle \times |n\rangle$ and $|X-Cr\rangle \times |n-1\rangle$, degenerated at resonance, are no longer stationary solutions of the hamiltonian. Instead, stationary solutions are anti-linear (noted $|I, n\rangle$ in Fig. I.16) and linear ($|II, n\rangle$) combination of the unperturbed states, split proportionally to the Rabbi flopping frequency Ω_r. This splitting is called Autler-Townes splitting and is well described by the dressed-atom picture.

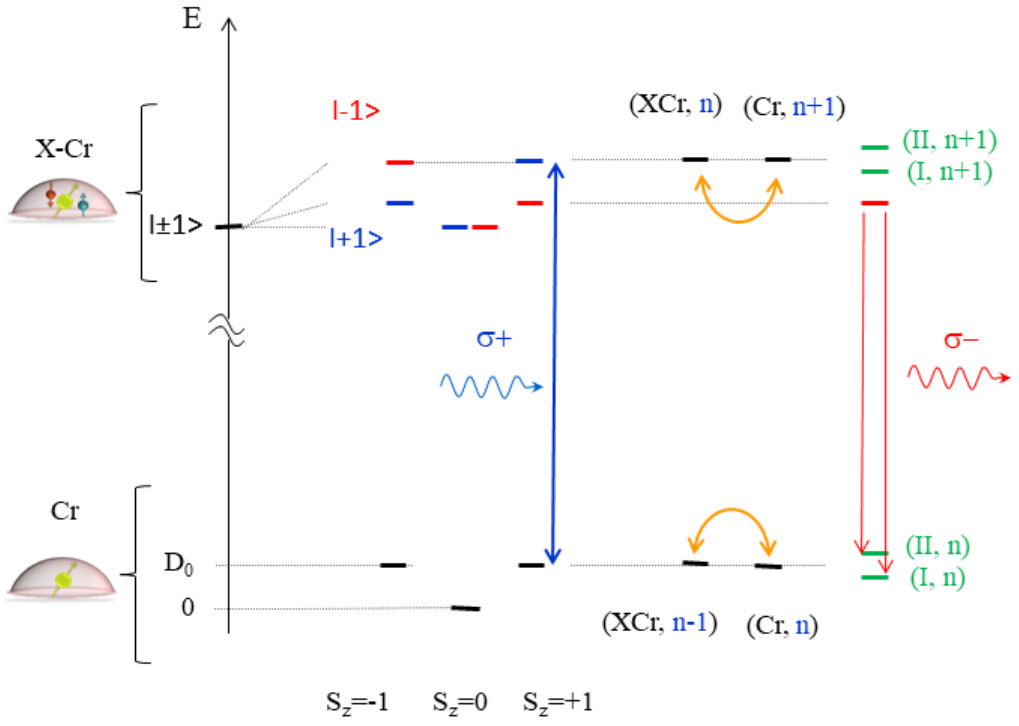

Figure I.16: Illustration of the energy level of a Cr-doped quantum dot and formation of the dressed-states.

In the dressed-atom formalism, the dressed state and the energy splitting are found using a quantum description of the QD levels and the laser field. We make the assumption that the Rabbi splitting Ω_r and the laser detuning δ are small compared to the splitting between two PL lines of the quantum dot. We can then calculate the dressed states resulting from the interaction between the two levels of the QD addressed by the laser, noted $|G\rangle$ for the ground state and $|E\rangle$ for the excited state, and the resonant laser photons, neglecting the light-matter interaction of all the other levels. An illustration of such a system is given in Fig. I.16 for $|G\rangle = |Cr\rangle$ and $|E\rangle = |X - Cr\rangle$, with $S_z = +1$ and $X_z = +1$.

In the absence of coupling between the two considered states, the Hamiltonian of this two level system is written:

$$\mathcal{H}_{AT}^{unpert} = \hbar\omega_L pp^\dagger + \hbar\omega_{EG}|E\rangle\langle E| \tag{I.4}$$

with p (resp. $p^\dagger$) is the annihilation (resp. creation) operator for a photon in the mode ω_L. The eigenstates of this system are $|G, n\rangle$, with the energy $\hbar n\omega_L$, and $|E, n\rangle$, with the energy $\hbar(\omega_{EG} + n\omega_L)$. Since the detuning $\delta = \omega_L - \omega_{EG}$ is many order of magnitude smaller than ω_L and ω_{EG}, the energy level are grouped two by two. The energy levels are then organized in doublet, formed by the states $|G, n\rangle$ and $|E, n-1\rangle$, split by δ. The doublet are seperated from each other by $\hbar\omega_L$. The states are represented in Fig. I.16 by (Cr, n), (XCr, n), $(Cr, n+1)$ and $(XCr, n+1)$, for $\delta = 0$.

The light-matter interaction originates for the dipole interaction. In second quantification, in the rotating wave approximation, it is written:

$$V \approx \hbar g(p|E\rangle\langle G| + p^\dagger|G\rangle\langle E|) \tag{I.5}$$

with g the electric dipole matrix element describing the couplig between the dipole of a QD transition and the mode ω_L of the electric field. The levels $|G, n\rangle$ and $|E, n-1\rangle$ of a multiplet are coupled through stimulated emission ($p^\dagger|G\rangle\langle E|$) and absorption ($p|E\rangle\langle G|$) of a photon. The total hamiltonian write for a given n photon state:

$$\mathcal{H}_n = \begin{pmatrix} \hbar n\omega_L & \frac{\hbar\Omega_{r,n}}{2} \\ \frac{\hbar\Omega_{r,n}}{2} & \hbar(\omega_{EG} + (n-1)\omega_L) \end{pmatrix} \tag{I.6}$$

with $\Omega_{r,n} = g\sqrt{n}$ is the Rabi frequency and $\delta = \omega_L - \omega_{EG}$ the detuning of the laser. We write the mean energy of the n photon state multiplet $E_n^0 = \frac{\hbar}{2}(\omega_{EG} + (2n-1)\omega_L)$. The hamiltonian $\mathcal{H}_n$ becomes:

$$\mathcal{H}_n = E_n^0 I_2 + \frac{\hbar}{2}\begin{pmatrix} \delta & \Omega_{r,n} \\ \Omega_{r,n} & \delta \end{pmatrix} \tag{I.7}$$

Diagonalizing the hamiltonian, we find the eigenstates $|I,n\rangle$ and $|II,n\rangle$ described at the beginning of this section:

$$|I,n\rangle = c|G,n\rangle - s|E,n-1\rangle \tag{I.8}$$
$$|II,n\rangle = c|G,n\rangle + s|E,n-1\rangle \tag{I.9}$$

with $c = \sqrt{\frac{1}{2}\left(1 - \frac{\delta}{\Omega'_{r,n}}\right)}$ and $s = \sqrt{\frac{1}{2}\left(1 + \frac{\delta}{\Omega'_{r,n}}\right)}$, with $\Omega'_{r,n} = \sqrt{\Omega^2_{r,n} + \delta^2}$ the generalized Rabi flopping frequency. We also find the corresponding energies and the splitting of the states:

$$E_I = E^0_n - \frac{\hbar}{2}\Omega'_{r,n} \tag{I.10}$$
$$E_{II} = E^0_n + \frac{\hbar}{2}\Omega'_{r,n} \tag{I.11}$$
$$\Delta E_{I-II} = \hbar\Omega'_{r,n} \tag{I.12}$$

At resonance ($\delta = 0$), $c = s = \sqrt{\frac{1}{2}}$. The states $|E,n-1\rangle$ and $|G,n\rangle$ corresponding to the upper and lower levels of the transitions have then equal contribution to the dressed levels $|I,n\rangle$ and $|II,n\rangle$: the dressed states are entangled atom-field states.

The splitting observed experimentally is given by $\Omega'_{r,n}$, with n the average number of photons of the laser excitation. This splitting depends on the Rabi splitting $\Omega_L = g\sqrt{n}$. Since n is proportional to the laser power P, Ω_L is then proportional to $\sqrt{P}$. In the following experiments, we observe it using a non resonant excitation to generate PL by a transitions involving a third level and an optically dressed state as shown in Fig. I.16. The PL of such a transition are split because, for instance, the emission from $|S_z = -1, +1\rangle$ can occur toward any of the dressed states (II,n) and (I,n) as they contain the component of the $|+1\rangle$ state. The resulting PL is split by Ω'_r: this is the Autler-Townes splitting [17]. In our QD, such a splitting can be observed in the PL of all the X-Cr states associated with $S_z = +1$: the low energy bright exciton state $|S_z = +1, -1\rangle$ (line (4)) and the dark exciton $|S_z = +1, +2\rangle$ (line (5)), close in energy to the bright exciton and which acquires some oscillator strength through the exciton mixing induced by the electron-hole exchange interaction in a low symmetry QD [7].

I.5.2 Dressing of a Cr atom

The Autler-Townes splitting could be exploited to control the coherent dynamics of a Cr spin [18, 19]. The optical configuration we use to observe it in a QD doped

with a single Cr atom is presented in Fig. I.17. When a high intensity single mode laser is tuned to the high energy line of X-Cr in $\sigma+$ polarization (X-Cr state $|S_z = +1, +1\rangle$), a splitting is observed in $\sigma-$ polarization in the PL of the two low energy lines produced by a second non-resonant laser. This is the same configuration as the one illustrated on Fig. I.16.

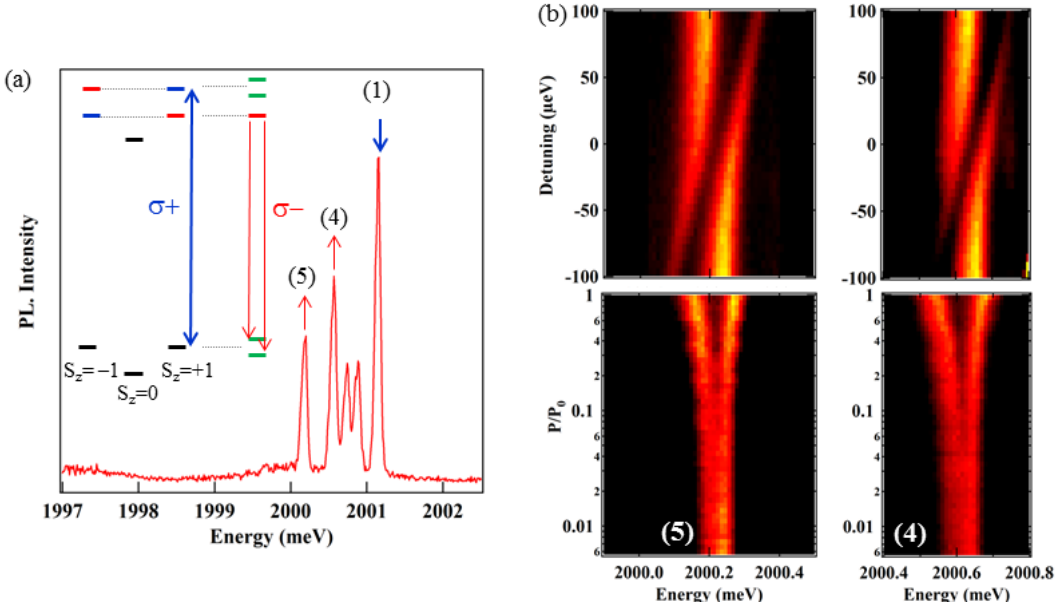

Figure I.17: (a) PL of QD2 X-Cr and configuration of excitation in the resonant optical control experiments. The inset illustrate the laser induced splittings in the ground and excited states for a $\sigma+$ excitation on $|S_z = +1\rangle$. (b) PL intensity maps of lines (5) and (4) for an excitation on (1) as a function of the detuning (top) and of the excitation intensity (bottom). The PL is produced by a second non-resonant laser.

Both the line (4) and line (5) are splitted in the same fashion by an excitation on line (1), showing that all those states share a common ground state. The splitting measured on line (5) for a resonant excitation on line (1) is plotted as a function of the square root of the resonant laser intensity P in Fig. I.18 showing that, as expected for a two level system, it linearly depends on the laser field strength. The Rabi splitting can reach 150 μeV at high excitation power. As the pump laser is detuned, the optically active transitions asymptotically approaches the original excitonic transitions where the remaining offset is the optical Stark shift.

A resonant laser permits to address any spin state of the Cr and selectively shift its energy. For instance, as presented in Fig. I.19, a $\sigma+$ excitation on the dark exciton state (5) induces a splitting of the high energy line (1) in $\sigma-$ polarization

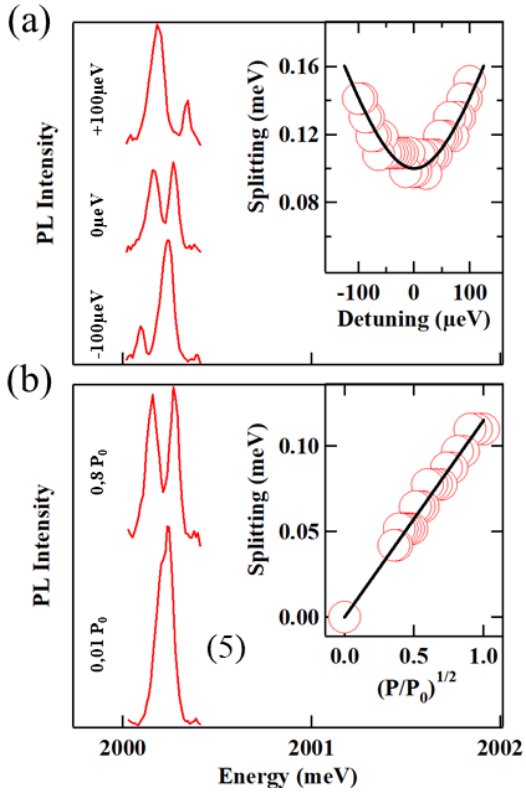

Figure I.18: PL spectra of line (5) for an excitation on line (1) at (a) no detuning and max detuning in each direction, and (b) low and high power. The insets show the splitting of the PL doublet as a function (a) of the laser detuning and (b) of the excitation intensity. The fit is obtained with $\hbar\Omega_r = 100$ μeV.

(state $|S_z = -1, -1\rangle$) without affecting the central line (2). This shows that such resonant excitation can be used to tune the energy of $S_z = -1$ without affecting $S_z = 0$. The energy tuning induced by a coherent optical driving is particularly interesting for the control of the Cr spin states $S_z = \pm 1$. These states could be efficiently mixed by applied weak anisotropic in-plane strain through a fine structure term of the form $E(S_x^2 - S_y^2)$ [7]. A relative shift of the energy of $S_z = +1$ or $S_z = -1$ by a resonant optical excitation would affect their coupling and consequently the Cr spin coherent dynamics.

Conclusion

The Cr spin dynamics was first probed using autocorrelation and crosscorrelation experiments, giving a relaxation time of the Cr spin τ_{Cr} of at least 20 ns.

In order to probe this dynamics with precision, we developed a pumping experiment for the Cr spin. Using resonant optical pumping, the Cr relaxation time in the dark was found to be $\tau_{Cr} = 1.7$ μs at T = 5 K. A relaxation channel between

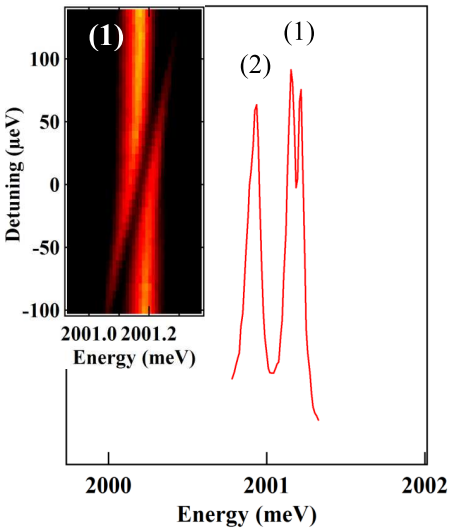

Figure I.19: PL of line (1) and (2) (high energy line) for a laser on resonance with the dark exciton state (5). Inset: PL intensity map of line (1) as a function of the laser detuning around (5).

the states $|S_z = \pm 1, X_z = \pm 1\rangle$ and $|S_z = 0, X_z = \pm 1\rangle$ were also evidenced by resonant optical pumping. We proposed a phonon-mediated h-Cr spin flip-flop to explain this relaxation, such as the one presented in Sec. III.2.3. It gives a hole-Cr relaxation time τ_{hCr} in the ns scale, which fits well the experiments.

We also show the possibility to control the Cr spin state using optical Stark shift. It is possible to independently tune each Cr spin state. It could therefore be used to affect the coupling of the different Cr states, especially the $S_z = +1$ and $S_z = -1$ states, coupled through the strain anisotropy term E.

Possible effects of the phonons on the Cr spin was also evidenced. However, the experiments conducted during this thesis was not enough to really conclude on these effects. Further experiments are needed to test them. We propose to deposit a thin metal layer on the back on the sample. A laser will then be able to excite phonons in it and inject them in the semiconductors without injecting carriers.

Bibliography

[1] P. Michler, A. Imamoglu, M. D. Mason, P. J. Carson, G. F. Strouse, and S. K. Buratto, "Quantum correlation among photons from a single quantum dot at room temperature", Nature **406**, 968 (2000).

[2] C. Santori, D. Fattal, J. Vuckovic, G. S. Solomon, and Y. Yamamoto, "Indistinguishable photons from a single-photon device", Nature **419**, 594 (2002).

[3] G. Sallen, A. Tribu, T. Aichele, R. Andre, L. Besombes, C. Bougerol, M. Richard, S. Tatarenko, K. Kheng, and J.-P. Poizat, "Subnanosecond spectral diffusion measurement using photon correlation", Nat Photon **4**, 696 (2010).

[4] A. Hundt, J. Puls, A. V. Akimov, Y. H. Fan, and F. Henneberger, "Photocarrier-induced spin heating and spin-lattice relaxation in diluted magnetic stranski-krastanov quantum dots", Phys. Rev. B **72**, 033304 (2005).

[5] M. K. Kneip, D. R. Yakovlev, M. Bayer, A. A. Maksimov, I. I. Tartakovskii, D. Keller, W. Ossau, L. W. Molenkamp, and A. Waag, "Direct energy transfer from photocarriers to Mn-ion system in II-VI diluted-magnetic-semiconductor quantum wells", Phys. Rev. B **73**, 035306 (2006).

[6] C. L. Cao, L. Besombes, and J. Fernández-Rossier, "Spin-phonon coupling in single mn-doped cdte quantum dot", Phys. Rev. B **84**, 205305 (2011).

[7] A. Lafuente-Sampietro, H. Utsumi, H. Boukari, S. Kuroda, and L. Besombes, "Individual Cr atom in a semiconductor quantum dot: optical addressability and spin-strain coupling", Phys. Rev. B **93**, 161301 (2016).

[8] C. Le Gall, R. S. Kolodka, C. L. Cao, H. Boukari, H. Mariette, J. Fernández-Rossier, and L. Besombes, "Optical initialization, readout, and dynamics of a Mn spin in a quantum dot", Phys. Rev. B **81**, 245315 (2010).

[9] E. Tsitsishvili, R. v. Baltz, and H. Kalt, "Exciton spin relaxation in single semiconductor quantum dots", Phys. Rev. B **67**, 205330 (2003).

[10] K. Roszak, V. M. Axt, T. Kuhn, and P. Machnikowski, "Exciton spin decay in quantum dots to bright and dark states", Phys. Rev. B **76**, 195324 (2007).

[11]L. Besombes, K. Kheng, L. Marsal, and H. Mariette, "Acoustic phonon broadening mechanism in single quantum dot emission", Phys. Rev. B **63**, 155307 (2001).

[12]G. Sallen, A. Tribu, T. Aichele, R. André, L. Besombes, C. Bougerol, M. Richard, S. Tatarenko, K. Kheng, and J.-P. Poizat, "Subnanosecond spectral diffusion of a single quantum dot in a nanowire", Phys. Rev. B **84**, 041405 (2011).

[13]L. Besombes and H. Boukari, "Resonant optical pumping of a Mn spin in a strain-free quantum dot", Phys. Rev. B **89**, 085315 (2014).

[14]C. Le Gall, A. Brunetti, H. Boukari, and L. Besombes, "Optical stark effect and dressed exciton states in a Mn-doped CdTe quantum dot", Phys. Rev. Lett. **107**, 057401 (2011).

[15]X. Xu, B. Sun, P. R. Berman, D. G. Steel, A. S. Bracker, D. Gammon, and L. J. Sham, "Coherent optical spectroscopy of a strongly driven quantum dot", Science **317**, 929–932 (2007).

[16]A. Muller, W. Fang, J. Lawall, and G. S. Solomon, "Emission spectrum of a dressed exciton-biexciton complex in a semiconductor quantum dot", Phys. Rev. Lett. **101**, 027401 (2008).

[17]S. H. Autler and C. H. Townes, "Stark effect in rapidly varying fields", Phys. Rev. **100**, 703–722 (1955).

[18]D. E. Reiter, V. M. Axt, and T. Kuhn, "Optical signals of spin switching using the optical stark effect in a mn-doped quantum dot", Phys. Rev. B **87**, 115430 (2013).

[19]S. Jamet, H. Boukari, and L. Besombes, "Spin dynamics of a mn atom in a semiconductor quantum dot under resonant optical excitation", Phys. Rev. B **87**, 245306 (2013).